GSA Data Repository 2017286

Fedortchouk et al., 2017, Three styles of diamond resorption in a single kimberlite: Effects of volcanic degassing and assimilation: Geology, doi:10.1130/G39066.1.

GSA Data Repository: Three styles of diamond resorption in a single kimberlite

DR1: Discriminating diamond resorption in kimberlite magma from resorption in the mantle

DR2: Samples and methods

DR3: Kimberlite petrography

DR4: Emplacement model of BK1 kimberlite pipe

DR1: Discriminating diamond resorption in kimberlite magma from resorption in the mantle

Morphological study of kimberlite-hosted diamonds (Zhang and Fedortchouk, 2012) shows that rounding of crystal edges and corners is a common dissolution feature of every diamond population shown by ~70% of diamonds, and is a product of resorption by reaction with the kimberlite magma (Fig. DR1-1). Development of ditrigonal shape of {111} faces is a common feature of kimberlite-induced resorption. However, rounded diamonds from pyroclastic kimberlites develop glossy surfaces, while those from coherent hypabyssal kimberlites typically show sharp corrosive features. Experiments replicated the glossy crystal forms by diamond dissolution in C-O-H fluid and the sharp features by dissolution in volatile-undersaturated melt (Fedortchouk et al., 2007). The remaining 10-20% of the diamonds exhibit a variety of resorption styles attributed by the authors to resorption in different mantle reservoirs while protected by the host mantle xenoliths (Fig. DR1-1).

In this study we confirm the above discrimination between kimberlite-induced and mantle-derived resorption by a combination of lines of evidence. In each kimberlite lithology, we recognized a unique resorption style shown by all octahedral diamonds with various degrees of rounding. We found the same resorption style on all diamonds attached to a piece of kimberlite that was not removed by initial acid cleaning (Fig. DR1-2C). The more resorbed sides of pseudohemimorphic diamonds that represent the interaction with the kimberlite magma show the same resorption style, while the other side that was protected by a xenolith/xenocryst remained unresorbed or preserved only mantle-derived resorption features (Fig. DR1-2B). Diamonds, which show a combination of two different resorption styles, have the same kimberlitic resorption style developed along the edges and corners, while mantle resorption is preserved in the middle of {111} faces (Fig. DR1-2A).

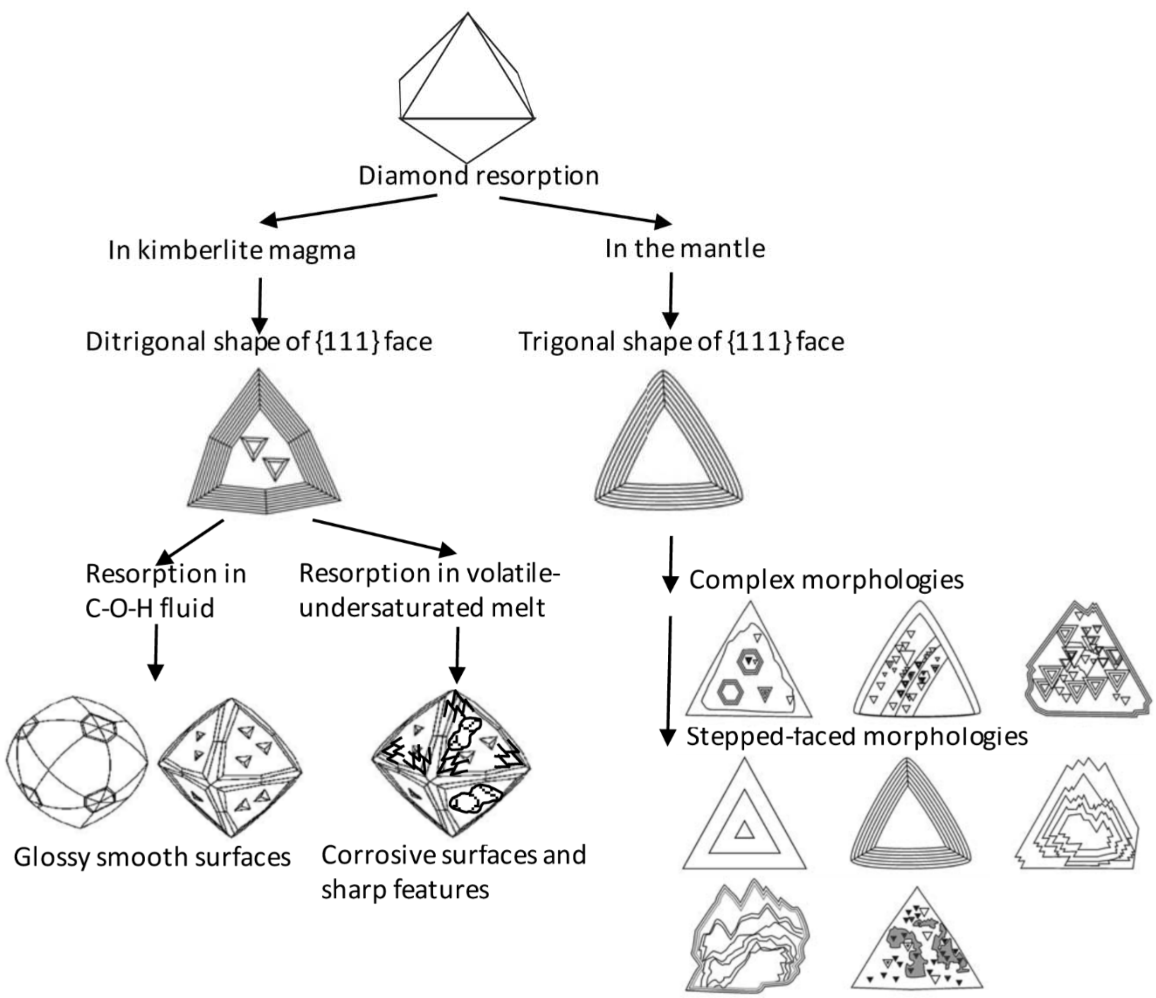

Figure DR1-1: Classification tree showing diamond resorption morphologies developed during resorption in kimberlite magma and in different mantle environments. Mantle resorption morphologies are from Zhang and Fedortchouk, 2012.

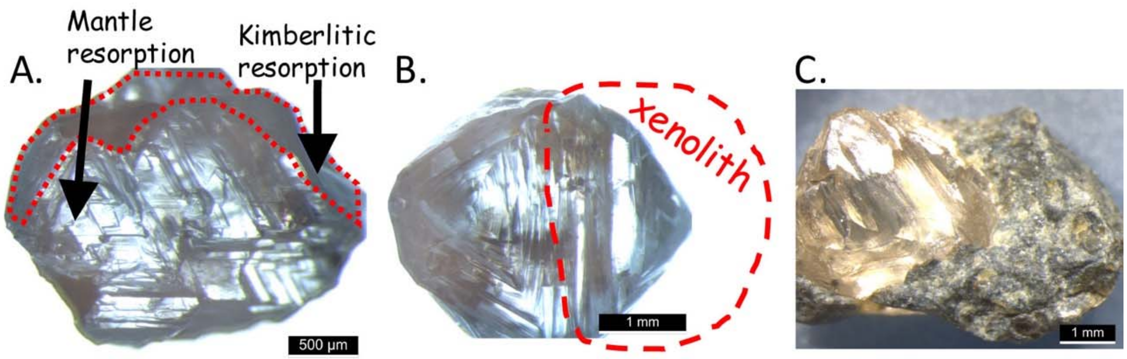

Figure DR1-2: A. Diamond combining two different resorption styles – one style on {111} faces and another style along the edges and in the corners; B. Pseudohemimorphic diamond with assumed previous extent of partially enclosing xenolith; C. Diamond attached to a piece of kimberlite.

DR2: Samples and methods

Diamond samples collected in drill hole intervals ranging from 2 – 13 m were examined separately and the collected diamond resorption data were combined for each ~ 40 m depth interval for statistical purposes (Table DR2-1 and Fig. DR2-2). All diamonds were sieved and examined under a stereo-microscope in reflected and transmitted light. The study used octahedral diamonds with different degrees of rounding, unbroken crystals and broken stones that preserved sufficient original morphology to allow discrimination of kimberlite-induced resorption from mantle-derived resorption. We studied the details of kimberlite-induced resorption using a Phenom ProX scanning electron microscope (SEM) with no coating of the diamonds. Kimberlite thin sections (70 from the depths of diamond recovery) were examined under a polarizing microscope; the groundmass mineralogy of representative samples was further studied using a SEM.

Among 802 studied diamonds, 496 diamonds have sufficient unbroken surfaces with resorption features to allow confident classification of these features as kimberlite-induced resorption, mantle-derived resorption, or an overprint of kimberlite-induced on mantle resorption. The proportion of unresorbed diamonds or those preserving mantle resorption (M) relative to the diamonds with kimberlite-induced resorption partially (K+M) or completely (K) overprinting any mantle-derived surface features is different in the three kimberlite lithologies in BK-1 and in the AK15 samples (Table DR2-1, Fig. DR2-2).

Table DR2-1: Distribution of diamonds with kimberlite-induced resorption (K), mantle-derived resorption (M), and combination of kimberlitic over mantle resorption (M+K) with depth in the three lithologies of BK1 kimberlite and in AK15 kimberlite.

Depth interval		Kimberlite Facies	Number of diamonds		Number of diamonds with resorption		
Sample From (m)	Sample To (m)		total studied	with assigned morphology	kimberlite-induced (K)	combined kimberlitic and mantle (K+M)	mantle-derived (M)
BK1: CK-A (DH 3)							
0	6	CK-A	4	1	1		
24	36	CK-A	7	5	2		3
36	41.3	CK-A	5	3	3		
41.3	48	CK-A	10	10	1	1	8
48	60	CK-A	15	12	4	2	6
60	72	CK-A	18	14	2	4	8
72	84	CK-A	11	8		3	5
84	96	CK-A	18	11	3	3	5
96	108	CK-A	18	13	1	2	10

108	120	CK-A	18	2	4	5	3
120	132	CK-A	27	15	2	7	6
132	141.9	CK-A	5	6	2	2	2
141.9	144	CK-A	6	6	0	3	3
144	156	CK-A	5	5	2	1	2
156	158.3	CK-A	1	1	0	1	0
158.3	163.8	CK-A	1	1	1	0	0
		Total	169	113	28	34	61
BK1: MVK (DH 2)							
4.3	11.7	CK-A	3	2	1		1
11.7	16.3	CK-A	3	1			1
16.3	28.3	CK-A	5	3			3
28.3	40.3	MVK	not described				
40.3	42.74	MVK	12	4			4
42.74	100.3	MVK	not described				
100.3	112.3	MVK	1				
112.3	124.29	MVK	21	13	5	1	7
124.29	136.29	MVK	19	8	4	1	3
136.29	148.3	MVK	29	4	4		
148.3	160.3	MVK	35	17	9	3	5
160.3	172.29	MVK	17	6	3	1	2
172.29	184.29	MVK	13	5	3		2
184.29	196.3	MVK	18	8	6	1	1
196.3	200	MVK	14	3	2		1
	Total		190	74	37	7	30
BK1: CK-B (DH 1)							
12	15.5	CK-B	2	2			2
15.5	24.47	CK-B	10	1	1		
27.5	39	CK-B	12	6		1	6
39	50.8	CK-B	4	2	1	1	
50.8	62.8	CK-B	4	3	2	1	
62.8	74.8	CK-B	5	4	3	1	
74.8	86.8	CK-B	10	10	6	1	3
86.8	98.8	CK-B	5	5	4	1	
98.8	110.8	CK-B	6	5	5		
110.8	122.8	CK-B	6	6	2	1	
122.8	134.8	CK-B	30	23	17	6	
134.8	146.8	CK-B	8	5	3	2	
146.8	158	CK-B	27	17	16		1
158	170.8	CK-B	17	11	8	2	1

170.8	182.8	CK-B	8	7	5	1	1
182.8	194.8	CK-B	9	7	7		
194.8	200	CK-B	9	8	7	1	
	Total		172	122	87	19	14
AK15							
0	2.67	CK	2	1		1	
2.67	7.04	CK	2	2	1		1
7.04	12	CK	1	1		1	
0	12	CK	6	5	3		2
12	19	CK	16	6	3	1	2
19	31	CK	54	31	16	8	7
31	43.04	CK	6	6	3	3	
43.04	46.88	CK	23	15	5	5	5
46.88	53.65	CK	not described				
53.65	55.04	CK	7	4	3		1
55.04	67.04	CK	44	33	21	5	7
67.04	79.04	CK	13	11	2	3	5
79.04	91.04	CK	22	18	8	4	6
91.04	103.04	CK	12	9	5		4
103.04	115.04	CK	29	15	2	2	11
115.04	119	CK	4	4	2		2
119	127.04	CK	16	6	2		4
127.04	139.04	CK	14	9	4	4	1
151.04	163	CK	1	1		1	
	Total		272	177	80	38	58

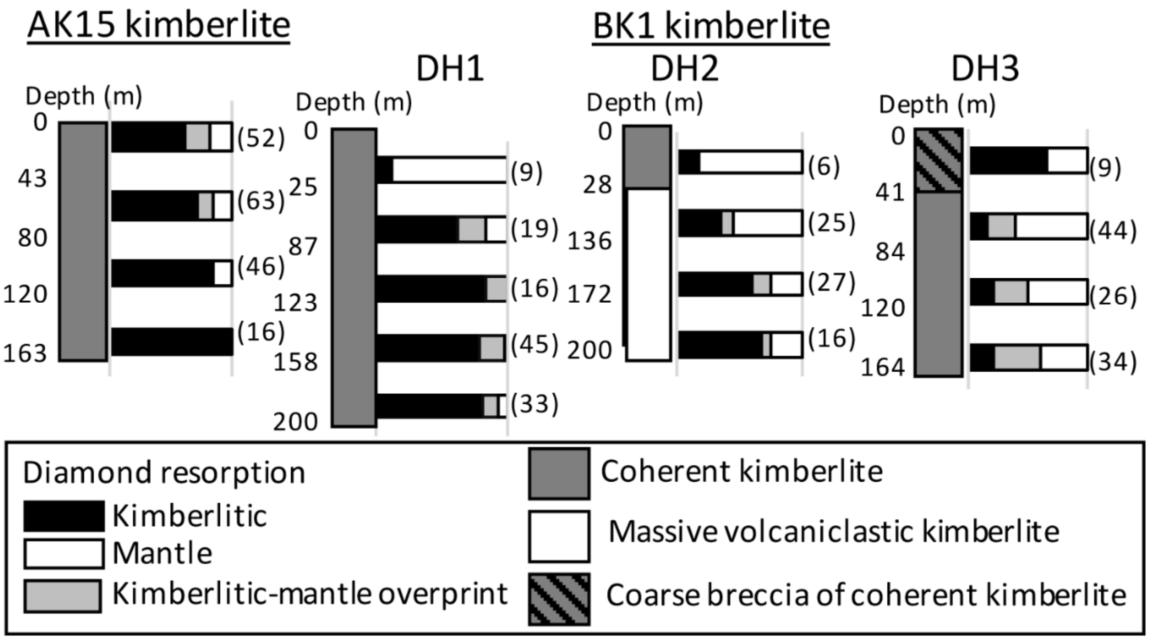

Figure DR2-2: A summary of drill hole logs and proportions of stones with kimberlite-induced, mantle-derived resorption, and combination of the two resorption styles with the sampling depth and kimberlite facies in three drill holes in BK1 and one drill hole in AK15. Numbers in brackets show the number of stones with assigned morphology at each sampling depth.

DR3: Kimberlite petrography

BK1 kimberlite pipe

Kimberlite CK-A is coherent kimberlite with segregationary texture of the groundmass and local development of diffuse oval juvenile clasts (Fig. DR3-1A). Serpentine segregations (1-10%) of irregular vermicular shape disrupt the groundmass into oval-shaped smaller and larger areas of the non-segregationary groundmass around macrocrysts (Fig. DR3-1A,B). These rounded areas resemble cored juvenile clasts, or pyroclasts, in volcaniclastic kimberlites, but show gradual, diffuse contacts with the adjacent serpentine segregations. Olivine macrocrysts

(15%) are replaced by serpentine or by carbonate in the core and serpentine on margins. The groundmass comprises 3% Ti-magnetite, 7% carbonate (may be secondary) and 90% serpentine (Fig. DR3-1A, B). Secondary, post-consolidation veins cutting through macrocrysts always make up 5-20% of the volume (Fig. DR3-1A). The veins are filled with carbonate + talc+/- serpentine. Groundmass comprises 90% serpentine, 7% carbonate, and 3%. Some olivine macrocrysts in CK-A (15%) show two stages of replacement, first by serpentine ± carbonate then to chrysotile ± Fe oxide minerals or to serpentine + talc.

The origin of CK-A is difficult to reconstruct. A gradual transition to the adjacent volcaniclastic kimberlite MVK and the presence of diffuse juvenile clasts which may be considered remnant pyroclasts match a possible reconstituted extrusive origin (van Straaten et al., 2011). At the same time, CK-A lacks angular shapes of olivine discrete crystals, non-uniform distribution of crystals and xenoliths and abundant non-assimilated country rock xenoliths typical of apparent coherent kimberlites with reconstituted extrusive origin (Hayman et al., 2008). Alternatively, CK-A may be a coherent kimberlite that experienced some volatile exsolution at a level not sufficient for complete volcanic fragmentation.

Kimberlite MVK is a pyroclastic kimberlite with textures transitional to coherent segregational. In places where the kimberlite demonstrates a classic pyroclastic texture, it contains 30% small oval magmaclasts, 20% serpentinized discrete olivines, 1% Ilm macrocrysts in the fine-grained matrix of serpentine, fibrous clinopyroxene and euhedral opaques (Fig. DR3-1D,E). The pyroclasts have serpentine cores and clinopyroxene rims; many of them look like classic “pelletal lapilli” (Mitchell, 1986) (Fig. DR3-1E), while other pyroclasts have double concentric rims (Fig. DR3-1E). MVK contains 10-30% of xenoliths and xenocrysts of Karoo basalts. Larger xenoliths preserved relic ophitic texture, while smaller xenoliths and xenocrysts are totally pseudomorphed by serpentine. The xenoliths are mantled by rims of fine grey fibrous clinopyroxene (Fig. DR3-1D). Rarely, phlogopite macrocrysts are resorbed and rimmed by clinopyroxene corona. Some large xenoliths are surrounded by a mantle of coherent kimberlite. In other areas where MVK kimberlite looks transitional, it contains diffuse juvenile clasts (10-20%) separated by serpentine segregations (10%) and the matrix of an opaque mineral (3%) and serpentine (Fig. DR3-1E).

Kimberlite CK-B (Fig. DR3-1C) is a coherent kimberlite with ~10-20% of olivine macrocrysts. Larger, ~1 mm macrocrysts are only partially (10-20%) serpentinized on their margins, whereas smaller microphenocrysts are entirely pseudomorphed by yellow serpentine (Fig. DR3-1C). The kimberlite contains 1-3% of totally digested Karoo xenoliths, which now look like patches of serpentine devoid of groundmass spinel. The groundmass is composed of 50% serpentine, 30% carbonate, 20% phlogopite, 3-15% perovskite and 3% Spl. Serpentine and carbonate form cryptocrystalline intergrowths, phlogopite is present in small colorless secondary (?) laths of random orientation.

AK15 kimberlite intrusion

AK15 kimberlite is a coherent kimberlite significantly contaminated by crustal xenoliths, mostly Karoo basalts. The studied AK15 thin sections represent a sequence from less contaminated (5% basalts) to more contaminated (60% basalts and 5% shales) kimberlites. The kimberlite contains 35-40% olivine and 1-2% phlogopite macrocrysts (Fig. DR3-1F). Smaller olivines range in shape from euhedral to angular, and some areas are enriched in small olivines compared to larger macrocrysts. Olivines are 90-100% replaced by colourless serpentine in relatively fresh kimberlite, but are pseudomorphed by serpentine and an unknown brown mineral in more altered samples (Fig. DR3-1F). The kimberlite has sergegationary texture, with segregations of carbonate (Fig. DR3-1F) or Carb+Serp. The groundmass is 60% serpentine, 10% phlogopite, 10% carbonate, 0-20% high relief globular light brown hydrogarnet, 0-30% fibrous clinopyroxene, 1% atoll spinel, 1% perovskite, an euhedral brown mineral (Fig. DR3-1F). Serpentine and carbonate form cryptocrystalline intergrowth, phlogopite is present in small colorless secondary (?) laths of random orientation.

Karoo basalts can be identified by ophitic texture preserved in some cores. Non-preserved, assimilated xenoliths are replaced by serpentine and carbonate in the core +/- possible bultfonteinite, +/- hydrogarnet and brown serpentine in the rim. A corona of fine clinopyroxene fibers grows radially on the xenoliths. In the inner part of the corona, the clinopyroxene is coarse and transparent, whilst in the outer parts of the corona clinopyroxene fibers form the grey mass of felt-like fibers (Fig. DR3-1F). Rare fibers of pectolite also occur. Shapes and sizes of totally digested xenoliths can be identified by the clinopyroxene coronas surrounding serpentine-hydrogarnet areas (Fig. DR3-1F). Assimilated xenoliths are replaced by small beige globules of hydrogarnet, which can reach almost 50% of the original xenolith volume (Fig. DR3-1F). Hydrogarnet is also present in the groundmass as a hybrid mineral mantling and replacing spinel and an opaque mineral. In contaminated areas, phlogopite margins are replaced by a fine black opaque mineral, serpentine and hydrogarnet (Fig. DR3-1F). The contaminated areas also show spinel replacement. The spinel forms atoll rings and the inner core is replaced by serpentine, while the marginal opaque rim survives (Fig. DR3-1F).

AK15 does not show petrographic evidence for a reconstituted extrusive origin, such as the presence of remnant pyroclasts, angular shapes of olivine discrete crystals (van Straaten et al., 2011), non-uniform distribution of crystals and xenoliths, the presence of minimally assimilated and reacted lithic clasts (Hayman et al., 2008). However, the geometry of the AK15 unit and the lack of gradual contacts with pyroclastic kimberlites would be the ultimate proof for a non-reconstituted origin of this coherent kimberlite.

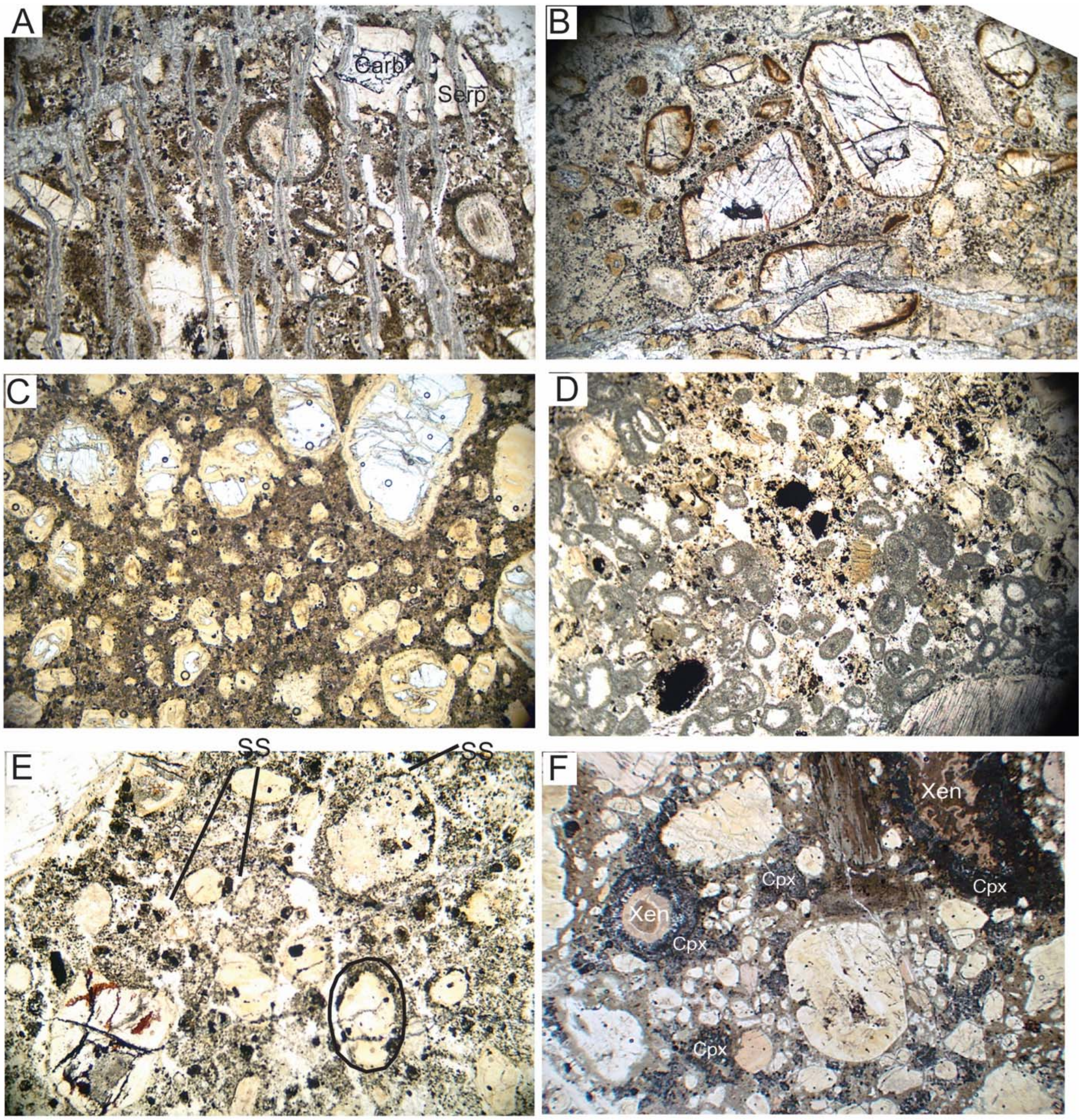

Figure DR3-1. A: General view of the CK-A kimberlite demonstrating segregationary texture, diffuse juvenile clasts, replacement of olivine by serpentine and carbonate and veins of carbonate and talc+serpentine (FOV 3 mm). B: Diffuse oval clasts (black dashed outline) cored by large olivine macrocrysts in CK-A kimberlite (FOV 3 mm). C: General view of the CK-B kimberlite demonstrating partially replaced olivine (FOV 3 mm). D: General view of MVK kimberlite demonstrating typical pyroclastic kimberlite texture, with multiple thin-skinned melt-coated oval clasts surrounded by fibrous grey clinopyroxene (FOV 6 mm). E: Local variation of the MVK kimberlite transitional to CK. Diffuse rounded clasts (black outline) are separated by serpentine segregations (SS) (FOV 1 mm). F: General view of AK-15 kimberlite demonstrating its high abundance of olivine, and xenoliths of Karoo basalt replaced by serpentine, hydrogarnet, and carbonate, and surrounded by fibrous clinopyroxene (Cpx) (FOV 6 mm).

DR4: Emplacement model of BK1 kimberlite pipe

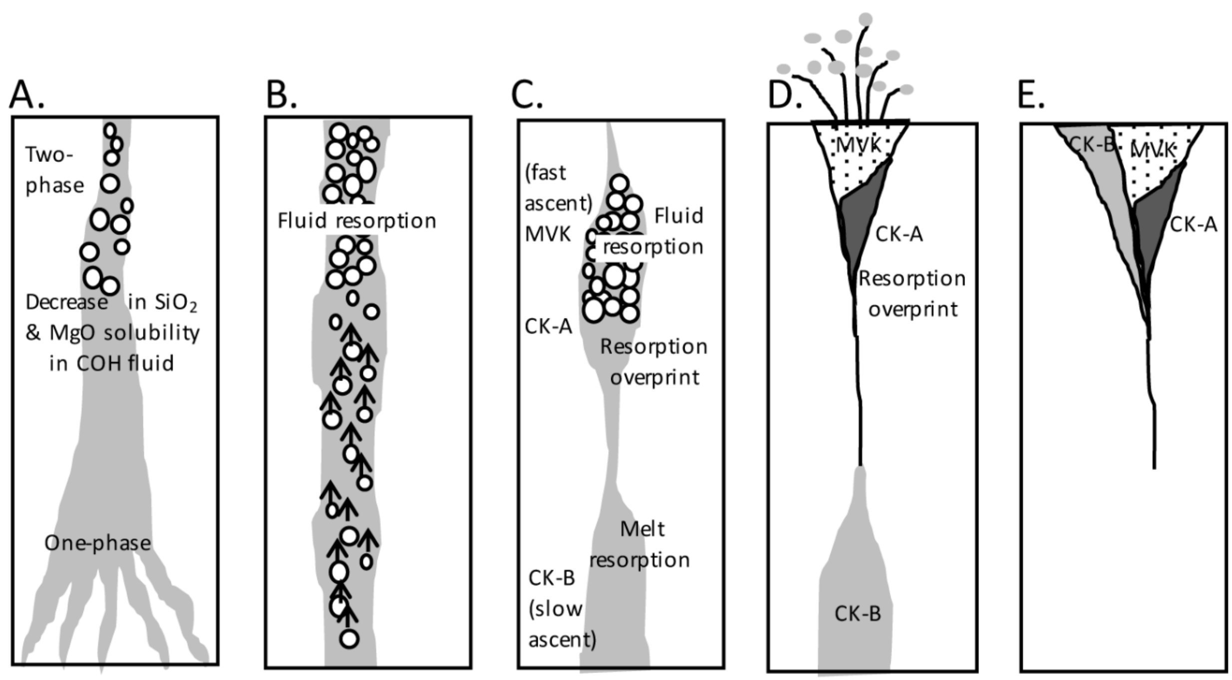

Figure DR4-1: Proposed emplacement model of BK1 kimberlite: A – fluid exsolution from kimberlite magma at P> 1GPa (~30-40 km) and a fluid-induced diamond resorption (glossy rounded crystals); B –bubble rise relative to the magma accelerated by bubble growth; C –

separation of bubble-rich head with fluid-style (glossy) diamond resorption from volatile-depleted melt tail with melt-style (corrosive) diamond resorption. D – explosive emplacement of the fluid-loaded head, opening the pipe, filling it with fragmented MVK and more volatile-depleted coherent CK-A. E – quiet emplacement of slower volatile-poor CK-B.